ELSEVIER

Biochimica et Biophysica Acta 1279 (1996) 93–103

BBA Biochimica et Biophysica Acta

Conducting and voltage-dependent behaviors of potassium ion channels reconstituted from diaphragm sarcoplasmic reticulum: comparison with the cardiac isoform

Maryse Picher, Anne Decrouy [1], Eric Rousseau *

Le Bilarium, Department of Physiology and Biophysics, Faculty of Medicine, University of Sherbrooke, 3001, 12th Avenue North, Sherbrooke, QC, J1H 5N4, Canada

Received 25 July 1995; accepted 3 October 1995

Abstract

Sarcoplasmic reticulum (SR) K^+ channels from canine diaphragm were studied upon fusion of longitudinal and junctional membrane vesicles into planar lipid bilayers (PLB). The large-conductance cation selective channel ($\gamma_{max} = 250$ pS; $K_m = 33$ mM) displays long-lasting open events which are much more frequent at positive than at negative voltages. A major subconducting state about 45% of the fully-open state current amplitude was occasionally observed at all voltages. The voltage-dependence of the open probability displays a sigmoid relationship that was fitted by the Boltzmann equation and expressed in terms of thermodynamic parameters, namely the free energy (ΔG_i) and the effective gating charge (Z_s): $\Delta G_i = 0.27$ kcal/mol and $Z_s = -1.19$ in 250 mM potassium gluconate (K-gluconate). Kinetic analyses also confirmed the voltage-dependent gating behavior of this channel, and indicate the implication of at least two open and three closed states. The diaphragm SR K^+ channel shares several biophysical properties with the cardiac isoform: $g = 180$ pS, $\Delta G_i = 0.75$ kcal/mol, $Z_s = -1.45$ in 150 mM K-gluconate, and a similar sigmoid P_o/voltage relationship. Little is known about the regulation of the diaphragm and cardiac SR K^+ channels. The conductance and gating of these channels were not influenced by physiological concentrations of Ca^{2+} (0.1 μM–1 mM) or Mg^{2+} (0.25–1 mM), as well as by cGMP (25–100 μM), lemakalim (1–100 μM), glyburide (up to 10 μM) or charybdotoxin (45–200 nM), added either to the *cis* or to the *trans* chamber. The apparent lack of biochemical or pharmacological modulation of these channels implies that they are not related to any of the well characterized surface membrane K^+ channels. On the other hand, their voltage sensitivity strongly suggests that their activity could be modulated by putative changes in SR membrane potential that might occur during calcium fluxes.

Keywords: Diaphragm sarcoplasmic reticulum; Potassium ion channel; Striated muscle; (Heart)

1. Introduction

Cardiac and skeletal muscle contraction is initiated by a rapid release of Ca^{2+} ions from the SR which is triggered by an action potential propagated along the plasma membrane and the transverse tubules [1–3]. It has been proposed that Ca^{2+} release and uptake along contraction-relaxation cycles may be modulated by the SR membrane potential, and that movements of monovalent ions across the SR membrane would maintain electroneutrality [4–8]. Monovalent ion channels specific for K^+, Na^+, H^+ and Cl^- have been reported in skeletal [9–11] and cardiac [12–14] SR membranes. The PLB fusion technique coupled to voltage-clamp measurements [15] has been used to characterize the skeletal [15–22] and the cardiac SR K^+ channels [14,23–26]. It has been shown that the properties of ion channels reconstituted into artificial membranes are not significantly altered during the reconstitution procedure [27]. Considering the difficult task of studying the electrophysiological properties of intracellular membranes in situ, the PLB fusion technique represents an adequate way to analyse single-channel activities and to test specific factors suspected of being involved in their regulation [28].

To our knowledge, the diaphragm SR ionic channels have not yet been investigated. Mammalian diaphragm, which is anatomically and histologically classified as a

* Corresponding author. Fax: +1 (819) 5645399; e-mail: e.rousse@courrier.usherb.ca.

[1] Present address: Department of Physiology, Faculty of Medicine, University of Ottawa, 451 Smyth, Ottawa, ONT, K1H 8M5, Canada.

SSDI 0005-2736(95)00239-1

skeletal muscle, shares several functional properties with the cardiac tissue. For instance, they both contract rhythmically for life and must return at the end of each relaxation phase to a relatively constant resting tension position. Furthermore, their relaxation properties are sensitive to load [29] and can be altered by ryanodine [30], a specific probe of the SR Ca^{2+} channel [3,31,32]. Furthermore, in contrast to skeletal muscles, the excitation-contraction coupling (ECC) in diaphragm and cardiac muscles relies on extracellular calcium [33]. Consequently, it was of interest to investigate the electrical properties of the diaphragm SR membrane and to compare them with those of the cardiac SR.

In this paper, we report for the first time the preparation and the ryanodine binding of canine diaphragm SR microsomal fractions recovered from sucrose gradients. Using fractions enriched either in longitudinal or junctional SR membranes and the PLB fusion technique, we have recorded single- and multiple-channel activities indicating the presence of a large-conductance K^+ channel. Ionic selectivity, voltage dependency, thermodynamic and kinetic analyses are reported. We have also tested several K^+ channel modulators as well as divalent cations. Some properties of the diaphragm channel were compared to those of the cardiac SR K^+ channel. Part of these results have been presented in abstract form elsewhere [34].

2. Materials and Methods

2.1. Materials

AMP (adenosine 5′-monophosphate), cGMP (guanosine 3′:5′-cyclic monophosphate), dithiothreitol and proteinase inhibitors were obtained from Sigma (St. Louis, MO). AEBSF (4-(2-aminoethyl)benzenesulfonyl fluoride) was obtained from Boehringer Mannheim and phospholipids were purchased from Avanti Polar-lipids (Alabaster, AL). Charybdotoxin was bought from Alomone Labs (Jerusalem, Israel), lemakalim from SmithKline-Beecham Pharmaceuticals (Worthing, UK) and glyburide from Hoertch (Montreal, Canada). [^{3}H]Ryanodine was purchased from New England Nuclear (NEN-Dupont Canada) and cold ryanodine was kindly provided by Dr. L. Ruest, Department of Chemistry, University of Sherbrooke, Canada. Deionized water from a Millipore Ro-Milli-Q-UF system (18 ± 0.2 MΩ/cm^2) was used for preparing all buffer solutions. All other chemicals were commercial products of analytical grade.

2.2. Preparation of sarcoplasmic reticulum vesicles

Microsomal fractions enriched in SR vesicles were prepared from canine diaphragm using a method derived from the procedure initially proposed by Meissner and Henderson [35]. Canine diaphragms were obtained from mongrel dogs anesthetized with pentobarbital (40 mg/kg, i.v.) in accordance with canadian and international standards for animal use. They were homogenized in a buffer containing (μM): 100 NaCl, 5 Tris-maleate, 5 K-EGTA, 0.05 AEBSF, 2 dithiothreitol, 1 ascorbic acid, plus 1 μM pepstatin, 1 μM leupeptin and 2.5 UI/ml aprotinin (pH 6.8), and centrifuged at 7 500 rpm ($6000 \times g$) for 20 min at 4°C in a Type 16 rotor (Beckman). The supernatant was filtered through two layers of cheesecloth and centrifuged at 33 000 rpm ($90\,000 \times g$) at 4°C for 1 h 20 min in a Ti 35 rotor (Beckman). The pellet was resuspended in a buffer containing (mM): 300 sucrose, 600 KCl, 1 K-EGTA, 5 K-Pipes (pH 7.0). This crude fraction was either stored at −85°C or centrifuged overnight at 24 000 rpm ($80\,000 \times g$) through a discontinuous 25–45% (w/w) sucrose gradient at 4°C in a SW 28 rotor (Beckman). Six isovolumic fractions were recovered from the sucrose gradient, diluted in 1.5 volume of 0.4 M KCl, 5 mM K-Pipes, 0.1 mM EGTA, 0.1 mM $CaCl_2$ (pH 7.0) and sedimented by centrifugation at 40 000 rpm ($120\,000 \times g$) for 1 h 20 min at 4°C in a 42.1 Ti rotor (Beckman). The pellets were resuspended in 300 mM sucrose and 5 mM K-Pipes (pH 6.8), frozen in liquid nitrogen and stored at −85°C [36].

2.3. Biochemical assays

Protein concentrations were determined by the Lowry method [37] using bovine serum albumin as a standard. Ryanodine binding assays were performed using the procedure previously described [31] with slight modifications. Briefly, SR vesicles (100 μg of protein) from each fraction were incubated in the presence of [^{3}H]ryanodine (with or without nonradioactive ryanodine) for 90 min at 37°C in the presence of 50 μM free Ca^{2+} and 5 mM AMP. The mixture was then centrifuged twice and pellet radioactivity was determined by liquid scintillation. Specific [^{3}H]ryanodine binding was calculated by subtracting nonspecific binding (5 nM [^{3}H]ryanodine + 5 μM ryanodine) from total binding (5 nM [^{3}H] ryanodine alone). Free Ca^{2+} concentrations were calculated using an apparent stability constant of $1.543 \cdot 10^{-7}$ (pH 7.4) for Ca-EGTA buffers, along with computer programs published by Fabiato [38].

2.4. Bilayer formation and vesicle fusion

The planar lipid bilayers (PLB) were formed at room temperature from a lipid mixture containing phosphatidylethanolamine, phosphatidylserine and phosphatidylcholine in a ratio of 3:2:1 [14]. The final lipid concentration was 25 mg/ml dissolved in decane. A 250 μm diameter hole, drilled in a Delrin cup, was pretreated with the same lipid mixture dissolved in chloroform. Using a Teflon stick, a drop of the decane lipid mixture was gently spread across the aperture in order to obtain an artificial membrane. Membrane thinning was assayed by applying a triangular wave test pulse. Typical capacitance values were 150–300

pF. Aliquots of SR vesicles (10–60 μg of protein) were added to the *cis* chamber in proximity of the bilayer. The *cis* and *trans* chambers contained 250 and 50 mM K-gluconate, respectively, 1 mM $CaCl_2$ and 20 mM Tris-Hepes (pH 7.2), unless specified otherwise. The fusions were either spontaneous, or encouraged by applying negative holding potentials across the bilayer [13]. Following a fusion event resulting in single or multiple channel incorporation, subsequent fusions were prevented either by lowering the free $[Ca^{2+}]_{cis}$ to 10 μM (by addition of Tris-EGTA, pH 7.2) or by neutralizing the K-gluconate gradient.

2.5. Recording instrumentation and statistical analyses

The currents were recorded using a low noise amplifier (Dagan 3900), then filtered (cut off frequency 5 kHz) and recorded on a digital audiotape recorder through a pulse code modulation device (75 ES-SONY, Unitrade). The currents were simultaneously displayed on-line on a chart recorder (DASH II MT, Astro Med.) and an oscilloscope (Kikusui, 5020A). Current recordings were played back, filtered at 500 Hz and sampled at 2 kHz for storage on hard disk and for further analyses using a DTK-FEAT-5030 computer with programs kindly provided by Dr. M. Nelson, University of Vermont. The open probability values (P_o) were determined from data stored in 60 to 120 s duration files unless specified otherwise, and the half-threshold discriminator method was used. Applied voltages were defined with respect to the *cis* chamber, which was held at virtual ground. All bilayer experiments were performed at room temperature (22 ± 2°C). The average values are given as means ± S.E. and *n* represents the number of measurements. Regression curves were calculated by the least square method using the Windows version of the Sigma Plot program from Jandel Scientific.

3. Results

3.1. Characterization of the diaphragm SR membrane vesicles

Diaphragm muscle microsomal fractions were separated on a 25–45% sucrose gradient [39]. The F_I fraction (≈ 16% sucrose) was recovered on top of the gradient and was shown to consist of a heterogeneous population of vesicles, membrane ghosts and lipid droplets [36]. Fractions F_{II}-F_{VI} contained each sucrose interface, for average sucrose densities of 30%, 33%, 37%, 40% and 43%, respectively. More than 50% of the protein content was recovered in the F_{III}-F_{IV} sucrose fractions. The microsomal fractions were further characterized using [^{3}H]ryanodine as a specific ligand for the SR Ca^{2+} release channel [3,31,32]. The ryanodine receptors were preserved by the addition of proteinase inhibitors. Our experimental results, based on multiple determinations ($n = 7$) indicate that the diaphragm ryanodine receptors are more abundant in the F_{IV} (37% sucrose) fraction, followed by the F_{III} (33% sucrose) fraction (Fig. 1). The present ryanodine binding profile is almost identical to the profile we previously reported for the canine cardiac SR [40]. These enrichment profiles differ slightly from those of the skeletal SR, where the highest ryanodine binding was collected on 40% sucrose (F_V fraction) [36], despite the use of the same protocol. All the following experiments were conducted either on the F_{III} or the F_{IV} fractions which are believed to be enriched in longitudinal or junctional SR membranes, respectively.

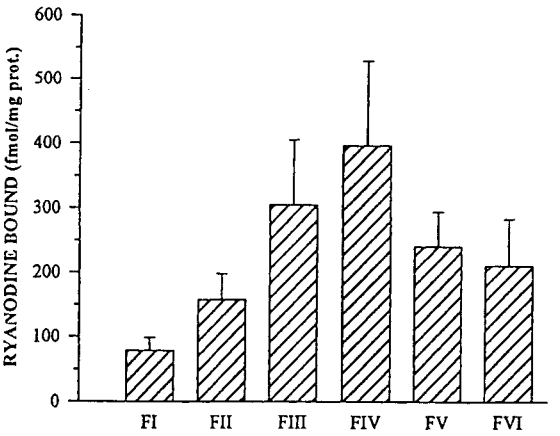

Fig. 1. [^{3}H]Ryanodine binding in the various vesicle populations of canine diaphragm recovered from 25–45% sucrose gradients. The F_I fraction (~ 16% sucrose) was recovered on top of the gradient. The fractions F_{II}-F_{VI} contain each sucrose interface for average sucrose densities of 30%, 33%, 37%, 40% and 43%, respectively. The highest level of [^{3}H]ryanodine was collected in fraction F_{IV}. The values represent the mean ± S.E. of 7 experiments performed in duplicate on different membrane preparations.

3.2. Identification of the canine diaphragm SR K^+ channel

Either single or multiple SR K^+ channel activities were recorded upon fusion of SR vesicles into PLB. Despite the fact that 85% of the fusions resulted in multiple channel recordings, it was possible to record single channel activities. Fig. 2A shows current fluctuations of a single channel as a function of the voltage applied across the bilayer in symmetrical 250 mM K-gluconate buffered solutions. At positive voltages, the channel displayed long-lasting open events, whereas negative voltages generated much fewer events, detected as downward deflections (lower trace). Such behavior has been reported for skeletal [41] and cardiac [14] SR K^+ channels. Well resolved subconducting states at 45% the current amplitude of the fully-open state were occasionally observed at all voltages. The amplitude histogram analysis (Fig. 2B) allowed the determination of the mean current values of the conducting states, as well as the open probability (P_o), which represents the fraction of time spent by the channel in the fully-open and subcon-

ducting states. For instance, at +60 mV, the P_o was equal to 0.81. The first peak corresponds to the zero-current level of the channel in its closed state. The small peak corresponds to the presence of subconducting states, with a mean gaussian amplitude of 7 pA, while the large peak corresponds to the current generated by the channel in its fully-open state, with a mean gaussian amplitude of 12.5 pA. At positive voltages, the fully-open and subconducting states predominated, whereas at negative voltages, the closed and fully-open states predominated. The overall contribution of the subconducting state represented less than 5% ($P_o < 0.05$) of the total open time.

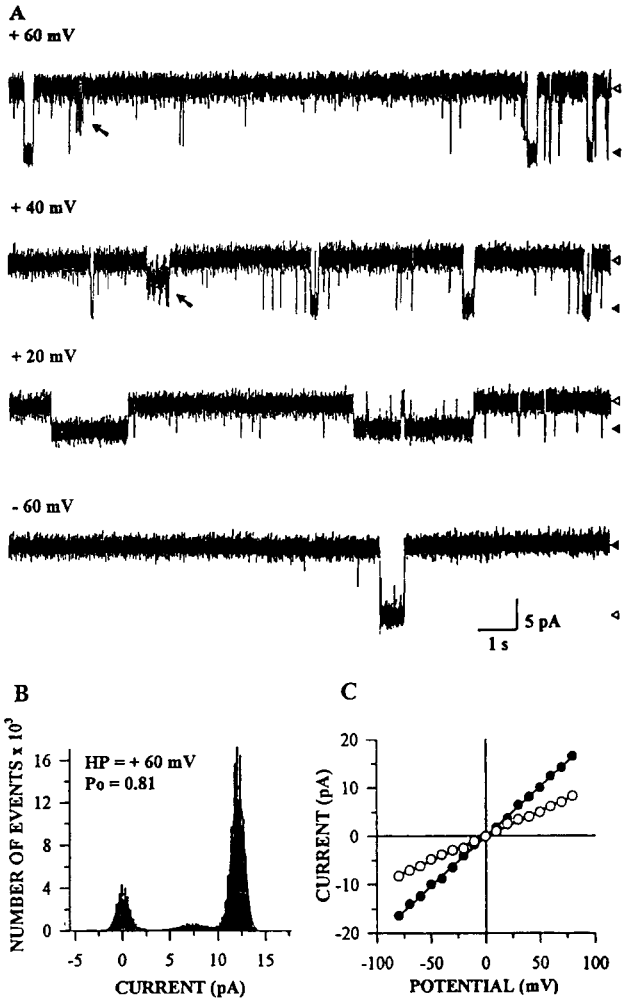

Fig. 2. Unitary currents of diaphragm SR K^+ channels as a function of the voltage. (A) Steady state current traces recorded at various holding potentials in symmetrical 250 mM K-gluconate + 1 mM $CaCl_2$ + 20 mM Tris-Hepes at pH 7.2. *Cis* to *trans* K^+ currents are shown as upward deflections. Triangles on the right indicate the fully-open (◁) and the closed states (◀), and arrows indicate subconducting states. (B) Amplitude histogram from a current trace obtained at +60 mV. $P_o = 0.81$ represents the fraction of time spent by the channel in the fully-open and subconducting states. The first peak corresponds to the zero current level of the channel in its closed state. The small peak corresponds to the subconducting state, with a mean current amplitude of 7 pA, and the large peak corresponds to the fully-open state, with a mean current amplitude of 12.5 pA. (C) Current/voltage relationships for the fully-open (●) and subconducting (○) states of the diaphragm SR K^+ channel in symmetrical 250 mM K-gluconate, corresponding to conductances of 210 pS and 97 pS, respectively.

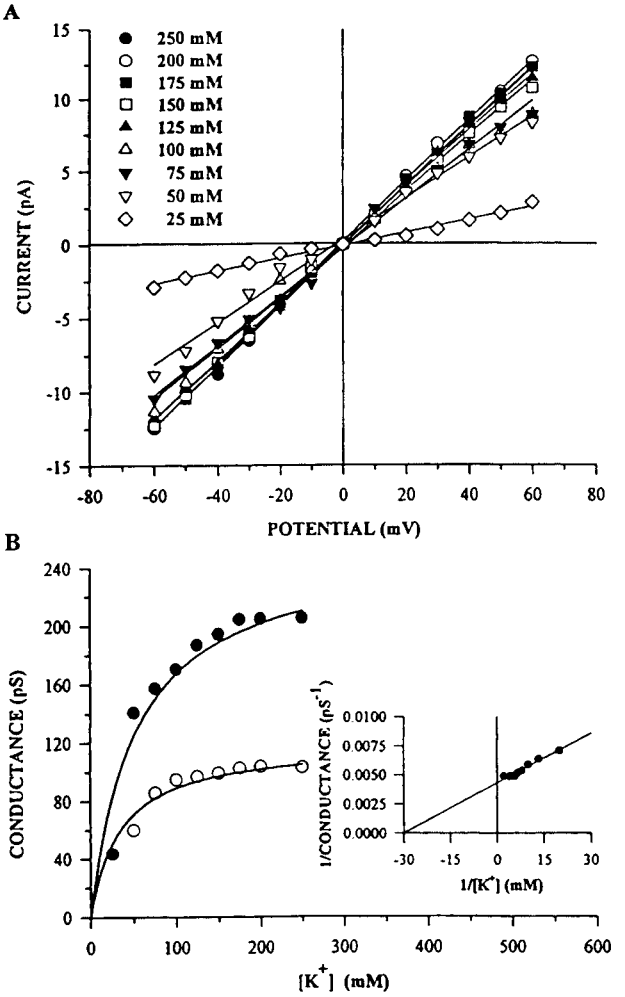

Fig. 3. Unitary conductances of diaphragm SR K^+ channels in symmetrical K-gluconate. (A) Mean current/voltage relationships for symmetrical K^+ concentrations ranging from 25 to 250 mM ($n = 4$ to 8). Subconducting current levels as well as error bars were omitted from this graph for clarity. The latter never exceeded 7% of the mean values. (B) Average unitary conductance values as a function of the K^+ concentrations for the fully-open (●) and subconducting (○) states. (Inset) Rearrangement of the data in the form of a Lineweaver-Burk plot indicates a maximal conductance of 250 pS and a K_m of 33 mM K^+.

3.3. Channel conductances and selectivity

Fig. 2C demonstrates that the current/voltage relationships were ohmic for both levels of open state in the range ±80 mV. In symmetrical 250 mM K^+, the unitary conductances were estimated at 210 pS and 97 pS for the fully-open and the subconducting states, respectively. A series of mean current/voltage relationships were built in symmetrical K-gluconate buffers, ranging from 25 to 250 mM (Fig. 3A). A replot of each average unit conductance as a function of K-gluconate concentration demonstrates

that the conductance of the channel starts to saturate around 210 pS, corresponding to 200 mM K^+ (Fig. 3B). Rearrangement of the data in the form of a Lineweaver-Burk plot indicates that the maximal conductance of the SR K^+ channel is 250 pS and the concentration of K^+ needed to reach half the maximal conductance (K_m) is 33 mM (Fig. 3B; inset).

Asymmetrical K-gluconate buffer systems were used to study the diaphragm SR K^+ channel selectivity. The reversal potential, which was close to zero in symmetrical conditions, was shifted toward negative voltages in asymmetrical buffer systems (25 to 250 mM *trans*/250 mM), and shifted toward positive voltages when the gradient was inverted (350 to 450 mM *trans*/250 mM), which argues in favor of a K^+ selectivity for this cation-conducting channel with respect to gluconate. Although the subconducting state was not included for clarity, the reversal potentials of the fully-open and the subconducting states were similar in each K-gluconate gradient, attesting that both states display the same selectivity. Fig. 4B illustrates the semi-logarithmic plot of the experimental reversal potentials (RP) as determined in Fig. 4A and the theoretical equilibrium potentials (E_k) as a function of K^+ concentrations in the *trans* chamber. The E_k values were calculated according to the Nernst equation. The two slope coefficients were not identical, suggesting that the large-conductance channel was not very selective for K^+ over gluconate. An alternative explanation for this discrepancy would be that above 100 mM K-gluconate, the activity of the dissociated K^+ would be significantly different from its concentration, whereas above 100 mM K^+, the slope would be similar to the one of the theoretical curve. For instance, the ionic activity estimated from the activity coefficients was 80 mM for a K^+ concentration of 100 mM ($a_i = 0.80$).

Fig. 4C shows the current/voltage curves obtained for the diaphragm SR K^+ channel in asymmetrical KCl buffers (filled symbols). The unitary conductances, 161, 178, 181 and 197 pS for 50, 150, 250 and 350 mM *trans*/250 mM *cis* KCl, respectively, were comparable to those measured in K-gluconate buffers (see Fig. 3B, Fig. 4A). In symmetrical conditions (250 mM KCl *trans*/*cis*), the reversal potential was at 0 mV, while it was shifted toward negative voltages, −24 mV and −9 mV in 50 mM *trans*/250 mM *cis* and 150 mM *trans*/250 mM *cis* KCl, respectively. Conversely, the reversal potential was shifted toward positive voltages (+6 mV) when the gradient was inverted (350 mM *trans*/250 mM *cis* KCl). Moreover, the zero-current potential values determined in KCl buffers were similar if not identical to the ones determined in K-gluconate buffers (see Fig. 4B). Consequently, the characteristics of the K^+ channel were not influenced by the anion species. Nevertheless, data analyses in KCl were restricted to the positive voltage range to minimize the putative contamination by anionic currents. As a matter of fact, the experiments performed in KCl allowed to measure Cl^- conductances through the well characterized di-

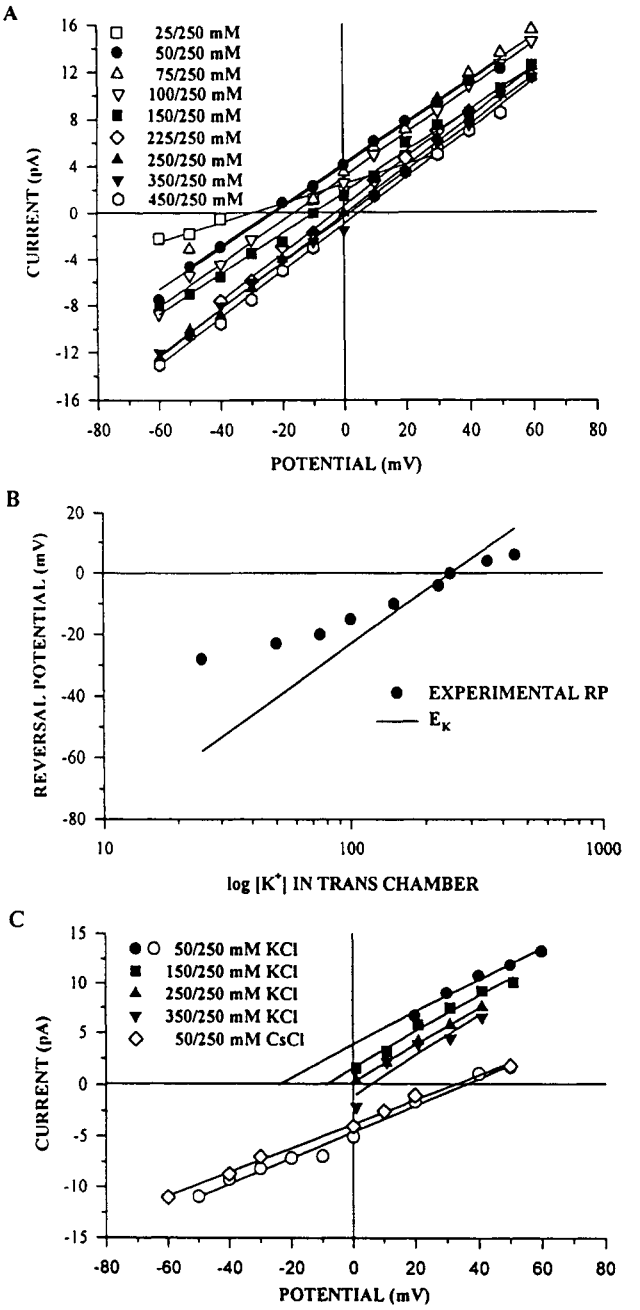

Fig. 4. Current/voltage relationships for diaphragm SR channels in asymmetrical buffered solutions. (A) Mean current/voltage relationship of the K^+ channel determined in the presence of K-gluconate 25 to 450 mM *trans*/250 mM *cis* ($n = 5$). Error bars were omitted on this graph for clarity, and never exceeded 5% of the mean values. (B) Semi-logarithmic plot of the experimental reversal potentials (RP) reported in (A) and the corresponding theoretical equilibrium potentials (E_k) as a function of K-gluconate concentration. E_k values were calculated with the Nernst equation at 22°C: $E_k = 58.52 \log ([K^+]_{cis}/[K^+]_{trans})$. (C) Current/voltage relationships of the K^+ channel in 50 to 350 mM *trans*/250 mM *cis* KCl (filled symbols), and current/voltage relationships of the Cl^- channel in 50 mM *trans*/250 mM *cis* KCl and CsCl (open symbols). Reversal potential of the K^+ channel was −24 mV. Reversal potentials of the Cl^- channel were +35 mV and +32 mV in KCl and CsCl, respectively.

aphragm SR Cl^- channel [34]. As shown in Fig. 4C (open symbols), the conductance of the Cl^- channel is lower than the conductance of the K^+ channel, with 129 pS and 119 pS in KCl or CsCl, respectively. Similar conductances were reported for cardiac [42] and skeletal [43,44] SR Cl^- channels. Moreover, the reversal potentials in 50 mM *trans*/250 mM *cis* KCl and CsCl were in the positive voltage range, with corresponding values of +35 mV and +32 mV.

The permeability ratio, P_{Cl}/P_K, calculated for the diaphragm SR K^+ channel from the Goldman-Hodgkin-Katz equation

$$E_{rev} = \frac{RT}{F} \ln\left(\frac{P_K[K]_o + P_{Cl}[Cl]_i}{P_K[K]_i + P_{Cl}[Cl]_o}\right) \quad (1)$$

was equal to 0.12, which demonstrates that the diaphragm K^+ channel is not very selective compared to the skeletal SR K^+ channel ($P_{Cl}/P_K = 0.02$) [45].

3.4. Voltage dependence of the open probability

The effect of transmembrane potential on the open probability of steady-state-activated channels was analysed. The open probability (P_o) of the diaphragm SR K^+ channel in symmetrical 250 mM K-gluconate was very high at voltages superior to +40 mV, and dropped rapidly to less than 0.20 at negative voltages (Fig. 5). The cardiac isoform also presented a similar sigmoid P_o/voltage relationship, with P_o values decreasing rapidly at voltages below +40 mV (data not shown). Thermodynamically, open-channel probability (P_o) can be expressed as a function of membrane potential (V_m) as follows [46]:

$$P_o = \left(1 + \exp\left(\left(\Delta G_i + Z_s F V_m\right)/RT\right)\right)^{-1} \quad (2)$$

where ΔG_i refers to 'internal free energy of opening', Z_s refers to 'effective gating charge', and F, R and T are the Faraday's constant, the gas constant and the absolute temperature, respectively. Eq. (1) can be rewritten as Eq. (2) in order to linearize the relationship:

$$\ln\left(\left(1 - P_o\right)/P_o\right) = \left(\Delta G_i + Z_s F V_m\right)/RT \quad (3)$$

Values of ΔG_i and Z_s can be determined from a plot of the left side of the equation vs. V_m (Fig. 5, inset). Mean ΔG_i was derived from the Y intercept at 0 mV (b) and the equation $\Delta G_i = bRT$, whereas mean Z_s was obtained from the slope (m) and the equation $Z_s = mRT/F$, at 22°C. For the diaphragm channels, ΔG_i was estimated at 0.27 kcal/mol K^+, and mean Z_s at −1.19, which corresponds to an e-fold decrease in P_o every 20 mV. For the cardiac isoform in symmetrical 150 mM K^+, mean ΔG_i was estimated at 0.75 kcal/mol K^+, and mean Z_s at −1.45, for an e-fold decrease in P_o every 18 mV.

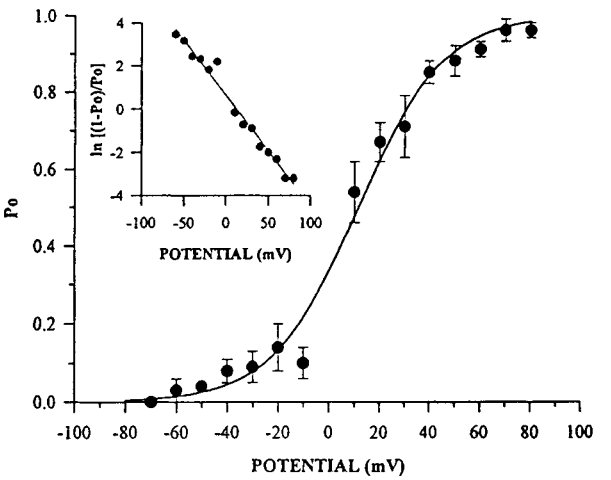

Fig. 5. Open probability as a function of the voltage for the diaphragm SR K^+ channel. Open probabilities (P_o) calculated from amplitude histogram analyses of single channel fusions recorded in symmetrical 250 mM K-gluconate. Values represent the mean ± S.E. of 7 fusion events. Note the voltage-sensitivity of the P_o. (Inset) Linearization of the P_o/voltage relationship using the Ehrenstein and Lecar equation: $\ln((1 - P_o)/P_o) = (\Delta G_i + Z_s FVm)/RT$). Effective gating charge (Z_s) was obtained from the slopes (m) and the equation $Z_s = mRT/F$, whereas the free energy (ΔG_i) was obtained from the Y intercept at 0 mV (b) and the equation $\Delta G = bRT$.

3.5. Channel kinetics

Time analyses of single channel fluctuations were performed in symmetrical 250 mM K-gluconate solutions at various potentials in order to formulate a simplified but plausible kinetic scheme for the SR K^+ channel. Time distribution histograms for the open and closed events were constructed with the half-threshold discriminator method (Fig. 6A–D). The number of exponentials needed to fit these distributions indicates whether the distribution arose from a single population of events or from the combination of distinct populations [47]. For instance, in the positive voltage range, the open time histograms were best fitted with the sum of two exponentials, suggesting the presence of two open states (Fig. 6A), whereas one exponential was sufficient to describe the closed time histograms, suggesting the presence of one closed state (Fig. 6B). In contrast, at negative voltages, the open time histograms were best fitted with one exponential (Fig. 6C), whereas the closed time histograms were fitted with two exponentials (Fig. 6D). Since only open or closed events shorter than 25 ms were considered for these intraburst analyses, long closed events were excluded from the time distribution. Despite their low frequency occurrence, these closed events of several seconds duration (as illustrated in Fig. 2A) are probably responsible for the very low P_o measured at negative voltages (see Fig. 5). Thus, the canine diaphragm SR K^+ channel would enter at least two open states and three closed states. Analyses performed on the diaphragm channel over a wide range of potentials in symmetrical 250 mM [K^+] demonstrate that the first open time constant ($\tau_{o,1}$) was basically voltage insensitive, whereas the second open time constant ($\tau_{o,2}$) increased by

2-fold at positive voltages (Fig. 7A). It was not possible to measure accurately the mean $\tau_{o,2}$ values in the negative voltage range because of the low P_o and low occurrence of long open events. Similarly, the first closed time constant ($\tau_{c,1}$) was voltage insensitive, but the second closed time constant ($\tau_{c,2}$) increased with membrane hyperpolarization (Fig. 7B). The cardiac SR K^+ channel was also found to display a similar gating behavior, including at least two open states and two closed states of comparable durations. For instance, open time constants at +30 mV in 400 *cis*/50 *trans* mM K-gluconate were $\tau_{o,1} = 0.8$ ms, $\tau_{o,2} = 27.7$ ms, $\tau_{c,1} = 0.6$ ms and $\tau_{c,2} = 4.2$ ms. The fact that membrane depolarization increases the channel's open probability (Fig. 5) as well as the duration of open events (Fig. 7A), and that hyperpolarization produces the opposite effects, supports the view that the SR membrane potential could fluctuate during Ca^{2+} cycling and thus regulate the counter-charge transport of monovalent cations.

3.6. Time-dependent activation and deactivation

Most vesicle fusions in the PLB resulted in multiple channel recordings, as previously reported for skeletal [19] and cardiac [23,48] SR K^+ channels. Consequently, square voltage steps were used to assess the time-dependent behavior of the diaphragm SR K^+ channels, when several of them were fused to the bilayer. Fig. 8A illustrates a typical voltage- and time-dependent activation of diaphragm SR K^+ channels, as well as their deactivation. All channels opened when the voltage was brought from 0 to +40 mV, with a mean half-time of 1.4 s ($n = 15$). They were then deactivated by a pulse from +40 to −40 mV with a mean half-time of 6.5 s ($n = 15$). Channel activation was systematically faster than deactivation, which follows the offset of the voltage pulse. These properties were observed independently of the K^+ concentration or the voltage pulse applied. The deactivation time courses were fitted with two exponentials corresponding to mean ($n = 10$) tau (τ) values of 5 ms and 2300 ms (Fig. 8B). A similar behavior was observed with the cardiac SR K^+ channel in asymmetrical buffer systems (250 *trans*/50 *cis* mM K-gluconate), with corresponding mean ($n = 12$) τ values of 22 ms and 1140 ms (data not shown). This type of time- and voltage-dependent channel gating behavior reinforces our proposition that these channels could be activated by a putative SR membrane depolarization and would become deactivated upon repolarization of the SR membrane.

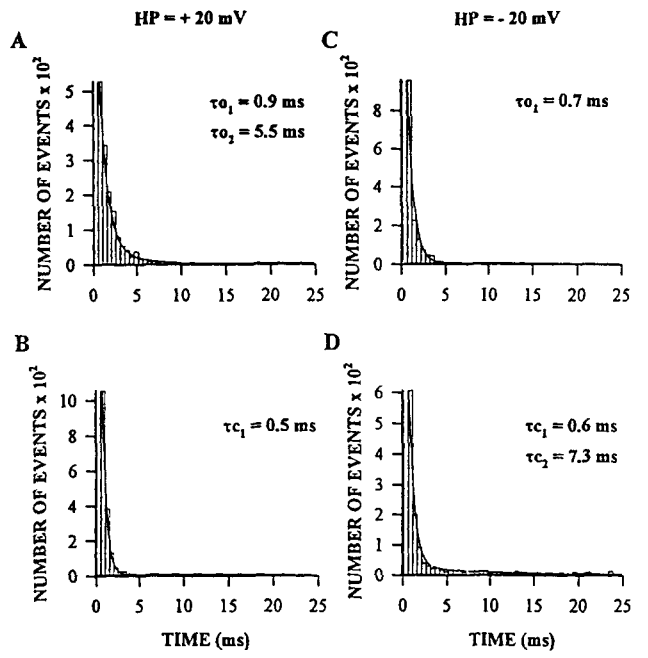

Fig. 6. Intraburst analyses of the diaphragm SR K^+ channel in the form of open and closed time histograms. (A) Open and (B) closed time distributions of a single channel recorded at +20 mV in symmetrical 250 mM K-gluconate. The open distribution was described by two exponentials with time constants of 0.9 and 5.5 ms, whereas the closed time distribution was described by a single exponential with a time constant of 0.5 ms. (C and D) Similar analyses at −20 mV. The open time distribution was best fitted with only one exponential with a time constant of 0.7 ms, whereas the closed time distribution required two exponentials of time constants equal to 0.6 and 7.3 ms ($T_{max} = 25$ ms).

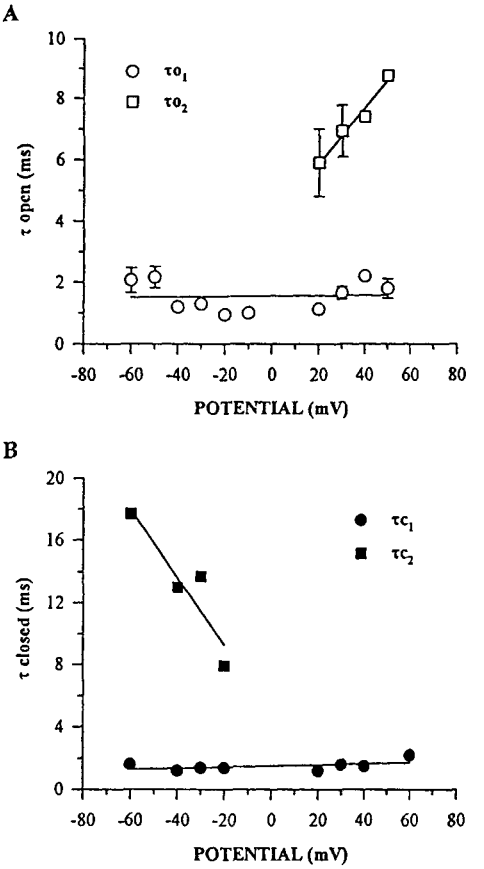

Fig. 7. Open and closed time constants as a function of holding potential. The values represent the mean ± S.E. of 8 experiments (A) $\tau_{o,1}$ was voltage insensitive, whereas $\tau_{o,2}$ increased with membrane depolarization. (B) $\tau_{c,1}$ was voltage insensitive, whereas $\tau_{c,2}$ decreased with membrane depolarization. The voltage dependency of $\tau_{o,2}$ and $\tau_{c,2}$ is consistent with the voltage-dependent behavior of the diaphragm SR K^+ channel.

3.7. Pharmacology of the SR K^+ channel

The diaphragm and cardiac SR K^+ channels were not modulated by physiological concentrations of Ca^{2+} (0.1 μM to 1 mM) or Mg^{2+} (10 μM to 0.5 mM) added either to the *cis* or the *trans* chamber. However, at +40 mV, 10 mM Mg^{2+} added to the *cis* chamber reduced the channels' current amplitude, and fully-open events were rarely observed (Fig. 9A). This effect was found to be concentration-dependent between 1 and 10 mM (Fig. 9B). However, no inhibition was reported at −40 mV, which suggests that the current reduction measured at +40 mV was caused by an asymmetrical blockage of the cation selective pore by mM $[Mg^{2+}]_{cis}$, as the K^+ diffused from the *cis* to the *trans* chamber.

In an attempt to relate these large-conductance K^+-selective channels to well characterized K^+ channels of the surface membrane, we have tested several compounds on the gating or the current amplitude. Lemakalim (100 μM), which is considered to be the most potent activator of ATP-activated K^+ channels [49–51], glyburide (10 μM), a selective blocker of ATP-dependent K^+ channels [52,53], charybdotoxin (45–200 nM), a known blocker of BK channels [54,55] and cGMP (25–100 μM), added either on the *cis* or *trans* side, all failed to modify the diaphragm and cardiac SR K^+ channels' properties (data not shown).

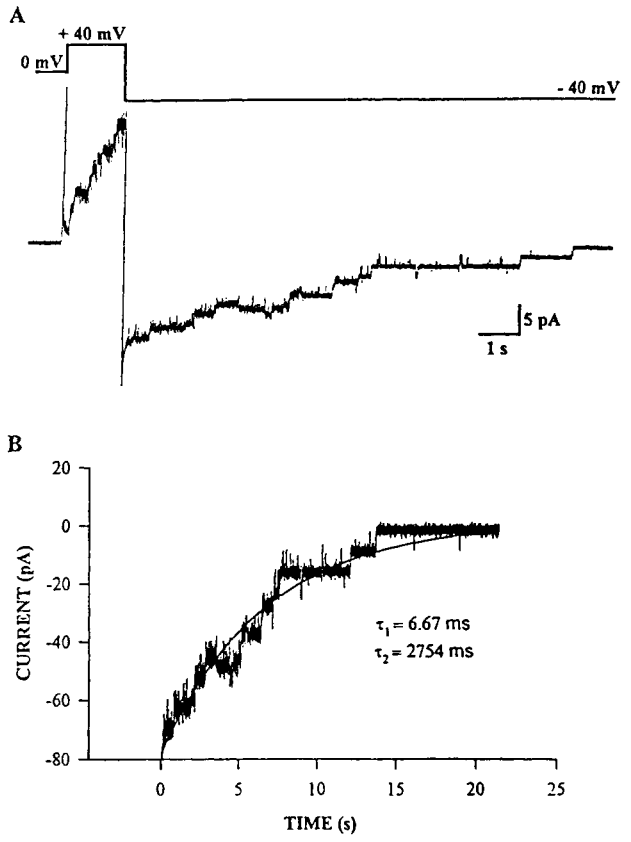

Fig. 8. Voltage-dependent deactivation of the diaphragm SR K^+ channels. (A) Multiple channel recording in 250 mM symmetrical K-gluconate. The channels were activated when the voltage was brought from 0 to +40 mV, and deactivated by a pulse at −40 mV. The capacitive current was removed from the analysis. Note that activation was more rapid than deactivation. (B) The deactivation time-course was fitted with the sum of two exponentials, with corresponding tau (τ) values of 6.67 ms and 2754 ms.

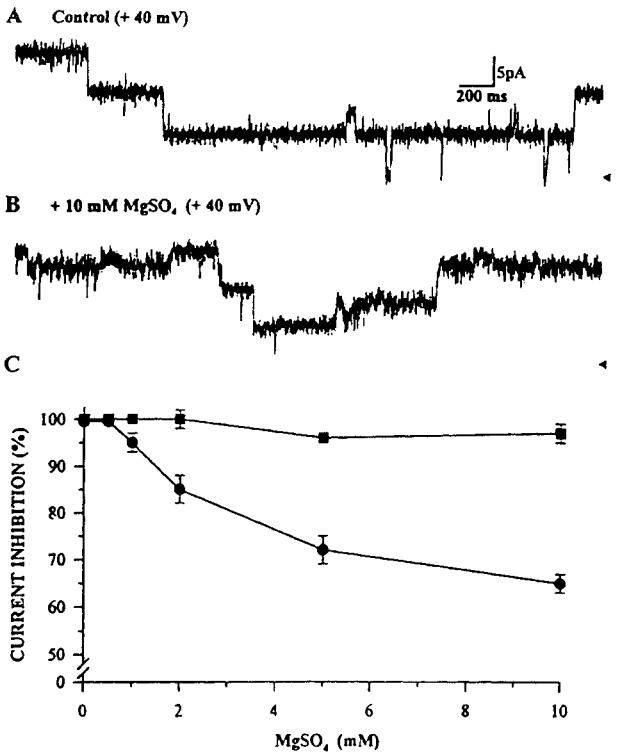

Fig. 9. Asymmetrical blockage of the diaphragm SR K^+ channels by mM $MgSO_4$. Two channels recorded in symmetrical 250 mM K-gluconate at +40 mV before (A) and after (B) the addition of 10 mM $MgSO_4$ to the *cis* chamber. Triangles on the right indicate the zero current level. (C) Percent inhibition of unitary current amplitude as a function of Mg^{2+} concentration at +40 mV (●) and −40 mV (■). Values represent mean ± S.E. of 8 experiments.

4. Discussion

The existence of a large-conductance K^+ channel in SR membranes has been clearly demonstrated in skeletal [17–19,43] and cardiac [23,25,48] muscles, and tentatively purified [25,43]. To our knowledge, the diaphragm SR ionic permeabilities have not yet been investigated. In this study, we have established the existence of a large-conductance K^+ channel in the diaphragm longitudinal and junctional SR membranes. This study defines the conducting properties as well as the voltage- and time-dependent behaviors of the diaphragm channel. Some of these properties are compared to those of the cardiac SR K^+ channel that we have previously partially described [14].

The diaphragm SR K^+ channel shares several biophysical properties with the skeletal [17–19] and the cardiac SR

K^+ channels [14,23–26,48,56,57]. Each potential applied across the artificial bilayer generates long-lasting open events and a main subconducting state ($P_o < 0.05$) of current amplitude at 45% that of the fully-open state. This subconducting state corresponds to the O_1 state, as defined by Hill et al. [23,48] in their previous report on the cardiac isoform. The channel exhibits an ohmic current/voltage relationship in the range ±80 mV, and a maximal unitary conductance of 250 pS, which is in the same range as reported for cardiac [22,23,25] and skeletal K^+ channels [20,56]. From the conductance/$[K^+]$ relationship, we have also determined a K_m value of 33 mM, which is about 1/4 of the intracellular K^+ concentration. These values are in agreement with the ones reported for mammalian skeletal SR K^+ channels, with $\gamma_{max} = 240$ pS and $K_m = 54$ mM [20]. For the cardiac SR K^+ channels in 400 *cis*/50 *trans* mM K^+, we measured γ_{max} and K_m values of 200 pS and 25 mM, respectively. Reversal potentials for the fully-open and the subconducting states were similar under various asymmetrical K-gluconate gradients, attesting that both states display the same selectivity. Similar conductances and reversal potentials were measured in asymmetrical K-gluconate and KCl buffers. A permeability ratio, P_{Cl}/P_K, of 0.12 was calculated, indicating that this K^+ channel was less selective than its skeletal muscle counterpart [45].

Amplitude histogram analyses demonstrate that at positive voltages, the fully-open and subconducting states predominate, whereas at negative voltages, the closed and fully-open states predominate, as reported for other SR K^+ channels [58,59]. The diaphragm and the cardiac SR K^+ channels presented very similar sigmoid-shaped P_o/voltage relationships that were fitted with the Boltzmann equation. Our previous studies involving the analysis of cardiac SR channels allow us to point out that the P_o/voltage relationship of the Cl^- channel [42] is inverted compared to the relationship determined for the K^+ channel. The Cl^- channel was found more active at negative than at positive voltages. The crossing-over between the two P_o/voltage curves occurs around 5 mV which, in the absence of direct electrophysiological measurements, corresponds to the best estimate of the SR membrane potential ($E_{SR} = 0$ to 7 mV) reported for the skeletal muscles [4,60]. This complementarity in P_o/voltage relationships suggests that the role of monovalent ionic and cationic conductances in the SR could be to maintain the membrane potential away from the Ca^{2+} equilibrium potential, and thus facilitate the rapid movements of Ca^{2+} during contraction-relaxation cycles, via the Ca^{2+} release channels and the Ca^{2+}, Mg^{2+}-ATPase. The putative functional cooperation between SR Cl^- and K^+ channels is currently being investigated in the canine diaphragm, in parallel with the immunological and biophysical study of the Ca^{2+} release channel [61].

The thermodynamic gating parameters obtained from a transformation of the P_o/voltage curves according to Ehrenstein and Lecar formalism [46] are in agreement with those obtained previously for the skeletal SR K^+ channel by Labarca et al. [62]. They noticed that in symmetrical buffer systems, the ΔG_i values were found to progressively decrease with increasing pH (values were as follows: pH 6, +1.56 kcal/mol; pH 7, +1.16 kcal/mol; pH 8, −0.73 kcal/mol). Our value of ΔG_i determined at pH 7.4 for the diaphragm was 0.27 kcal/mol K^+, which is in agreement with the trend. The effective gating charge, Z_s, was found by Labarca et al. [62] to be independent of external variables such as pH (values ranged between −0.80 and −0.92), and our value of −1.19 for the diaphragm channel is in the same order. Skeletal SR K^+ channels are also described by thermodynamic parameters which are in agreement with those of Labarca et al. [62]. For patch-clamp recordings of giant vesicle preparations of rabbit skeletal SR K^+ channels fused into planar membranes, $\Delta G_i = 0.95$ kcal/mol K^+ and $Z_s = -0.77$ at pH 7.2 [57]. The results we obtained for the canine cardiac SR K^+ channel in symmetrical 150 mM K^+ at pH 7.2 are $\Delta G_i = 0.75$ kcal/mol K^+ and a $Z_s = -1.45$. While the ΔG_i value follows the predictions of Labarca et al. [62], the Z_s value is higher than expected.

We must however mention that the equations derived by Ehrenstein and Lecar [46] to estimate the thermodynamic parameters assume the two-state (open and closed) model, which means that each channel has a single open and a single closed state [62]. The presence of subconductance states is of no concern, since their occurrence amounted to less than 5% of the total recording open time. Nevertheless, from our results on cardiac and diaphragm SR K^+ channels, and from those of Stein et al. [63] on skeletal muscle SR K^+ channels, it is becoming evident that these SR channels enter more than one open and one closed states. Channel kinetic analysis has revealed that the diaphragm SR K^+ channel enters at least two open and three closed states. Despite the fact that we have not ruled out the possibility that this channel may jump from long open to long-lasting closed events, the following scheme is proposed to summarize the channel's kinetics.

$$C_3 \rightleftarrows C_2 \rightleftarrows C_1 \rightleftarrows O_1 \rightleftarrows O_2$$

where O_1 and O_2 represent fully-open states, and C_1, C_2 and C_3 the different closed states. This pattern does not take into account the low-occurrence subconducting state ($P_o < 0.05$). Analyses of current fluctuations of the swine skeletal muscle SR K^+ channel indicate that the channel uses one open state and three closed states. The open time histograms were well fitted by a single exponential ($\tau = 36$ ms), while the closed time histograms were described by at least three exponentials with τ values of 3 ms, 23 ms and the other one on the order of seconds [61]. These values are on the same order of magnitude as those presented for the diaphragm channel (Fig. 7). We have also shown that one of the open and one of the closed time constants describing this channel, $\tau_{o,2}$ and $\tau_{c,2}$, are voltage sensitive

(Fig. 7A,B), suggesting that putative changes in the SR transmembrane potential could modulate the gating behavior of this channel. To investigate this possibility, we applied square voltage pulses to multiple channel recordings. All channels opened when the voltage was brought from 0 to +40 mV, with a mean half-time of 1.4 s, and they were all deactivated by a pulse from +40 to −40 mV with a mean half-time of 6.5 s ($n = 15$). Channel activation was systematically faster than deactivation, independently of the K^+ concentration or the voltage pulse applied. This type of behavior suggests that this channel would inactivate upon repolarization of the SR membrane. The deactivation time courses were fitted with two exponentials corresponding to mean ($n = 10$) τ values of 5 ms and 2300 ms (Fig. 8B). Similar results were obtained with the cardiac SR K^+ channels in asymmetrical buffer systems (250 *trans*/50 *cis* mM K-gluconate), with corresponding mean ($n = 12$) τ values of 22 ms and 1140 ms.

The conductance and gating of these channels were not influenced by physiological concentrations of Ca^{2+} (0.1 μM–1 mM) or Mg^{2+} (0.25–1 mM), as well as by cGMP (25–100 μM), lemakalim (1–100 μM), glyburide (up to 10 μM) or charybdotoxin (45–200 nM), added either to the *cis* or to the *trans* chamber. However, addition of 1 to 10 mM Mg^{2+} to the *cis* chamber reduced the channels' current amplitude. This inhibition was observed at +40 mV, but not at −40 mV, suggesting that free cytoplasmic Mg^{2+} might reduce the K^+ permeability of the SR. However, in vivo intracellular free Mg^{2+} concentrations are in the range of 250–600 μM. Considering that millimolar concentrations of Mg^{2+} are required to block the K^+ current, this channel does not fall into the category of the inward rectifier K^+ channels, and Mg^{2+} is not expected to play a key role in the regulation of SR K^+ permeability. In contrast, Mg^{2+} is known to modulate the gating behavior of the SR Ca^{2+} release channel [36]. On the other hand, we have demonstrated that the gating of the diaphragm SR K^+ channel is voltage-sensitive. The fact that membrane depolarization increases the channel's open probability (Fig. 5) and the duration of open events (Fig. 7A), and that hyperpolarization produces the opposite effects, support the view that the K^+ channels could be regulated by fluctuations in SR membrane potential occurring during Ca^{2+} cycling. These features, along with our previous studies on cardiac SR K^+ and Cl^- channels, support the idea that the role of these monovalent cation selective channels, instead of preserving electroneutrality [4–8], would be to maintain the SR membrane potential away from the Ca^{2+} equilibrium potential, and thus facilitate Ca^{2+} fluxes across the membrane during contraction-relaxation cycles.

Because of their apparent lack of biochemical or pharmacological regulation, it is not possible to relate the diaphragm and cardiac SR K^+ channels to any of the known families of K^+ channels. However, a polypeptide of 80 kDa was partially purified from canine cardiac SR membranes on sucrose gradient following CHAPS solubilization [25]. Upon reconstitution in the planar lipid bilayer system, this protein displayed the conductance and voltage-dependent gating behavior of the native cardiac SR K^+ channel. Since the cardiac and the diaphragm SR K^+ channels display similar biophysical properties, it might be postulated that the diaphragm SR K^+ channel is a close isoform of its cardiac muscle counterpart. The protein composition and structure of the diaphragm SR K^+ channel could provide valuable information on the physiological role and biochemical regulation of channel in striated muscles.

Acknowledgements

This study was supported by grants from HSFC and CRM of Canada. Dr. E. Rousseau is a senior FRSQ scholar. The authors would like to thank Dr. M.D. Payet for his valuable suggestions in preparing the manuscript, and S. Proteau for her technical assistance. Most data on the cardiac SR K^+ channel were gathered by Miss Hélène Chabot during her Masters' degree.

References

[1] Martonosi, A.N. (1984) Physiol. Rev. 64, 1240–1320.
[2] Lai, F.A., Erickson, H.P., Rousseau, E., Liu, Q.-Y. and Meissner, G. (1988) Nature 331, 315–319.
[3] Anderson, K., Lai, F.A., Liu, Q.-Y., Rousseau, E., Erickson, H.P. and Meissner, G. (1989) J. Biol. Chem. 264, 1329–1335.
[4] Oetliker, H. (1982) J. Muscle Cell. Motil. 3, 247–272.
[5] Meissner, G. (1983) Mol. Cell. Biochem. 55, 65–82.
[6] Baylor, S.M., Chandler, W.K. and Marshall, M.W. (1984) J. Physiol. (London) 348, 209–238.
[7] Caillé, J., Ildefonse, M. and Rougier, O. (1985) Progr. Biophys. Mol. Biol. 46, 185–239.
[8] Jdaïaa, H., Brûlé, G., Fournier, F. and Guilbault, P. (1989) Gen. Physiol. Biophys. 8, 39–56.
[9] Kometani, T. and Kasai, M. (1978) J. Membr. Biol. 41, 295–308.
[10] McKinley, D. and Meissner, G. (1978) J. Membr. Biol. 44, 159–186.
[11] Kasai, M., Kanemasa, T. and Fukumoto, S. (1979) J. Membr. Biol. 51, 311–324.
[12] Meissner, G. and McKinley, D. (1982) J. Biol. Chem. 257, 7704–7711.
[13] Rousseau, E. (1989) J. Membr. Biol. 110, 39–47.
[14] Rousseau, E., Chabot, H., Beaudry, C. and Muller, B. (1992) Mol. Cell. Biochem. 114, 109–117.
[15] Miller, C. and Racker, E. (1976) J. Membr. Biol. 30, 283–300.
[16] Miller, C. (1978) J. Membr. Biol. 40, 1–23.
[17] Coronado, R. and Miller, C. (1979) Nature (London) 280, 807–810.
[18] Coronado, R. and Miller, C. (1980) Nature (London) 288, 495–497.
[19] Coronado, R. and Miller, C. (1982) J. Gen. Physiol. 79, 529–547.
[20] Coronado, R., Rosenberg, R.L. and Miller, C. (1980) J. Gen. Physiol. 76, 425–446.
[21] Garcia, A.M. and Miller, C. (1984) J. Gen. Physiol. 83, 819–839.
[22] Tomlins, B., Williams, A.J. and Montgomery, R.A.P. (1984) J. Membr. Biol. 80, 191–199.
[23] Hill, J.A., Coronado, R. and Strauss, H.C. (1989) Biophys. J. 55, 35–46.

[24] Coronado, R. and Latorre, R. (1982) Nature (London) 298, 849–851.
[25] Liu, Q.-Y., Lai, F.A., Shen, W.K., Meissner, G. and Strauss, H.C. (1991) FEBS Lett. 291, 13–16.
[26] Uehara, A., Yasukohchi, M., Ogata, S. and Imanaga, I. (1991) Pflügers Arch. 417, 651–653.
[27] Miller, C. (ed.) (1986) Ion Channel Reconstitution, Plenum Press, New York.
[28] Smith, J.S., Coronado, E. and Meissner, G. (1986) J. Gen. Physiol. 88, 573–588.
[29] Hervé, P., Lecarpentier, Y., Brenot, F., Clergue, M., Chemla, D. and Duroux, P. (1988) J. Appl. Physiol. 65, 1950–1956.
[30] Zavecz, J.H. and Anderson, W.M. (1992) J. Appl. Physiol. 73, 30–35.
[31] Hawkes, M.J., Diaz-Munoz, M. and Hamilton, S.L. (1989) Membr. Biochem. 8, 133–145.
[32] Radon, D.P., Cefali, D.C., Mitchell, R.D., Seiler, S.M. and Jones, L.R. (1990) Circ. Res. 64, 779–789.
[33] Lecarpentier, Y., Péry, N., Coirault, C., Scalbert, E., Desche, P., Suard, I., Lambert, F. and Chemla, D. (1993) Am. Heart J. 126, 770–776.
[34] Rousseau, E., Michaud, C., Proteau, S. and Decrouy, A. (1995) Biophys. J. 68, A45.
[35] Meissner, G. and Henderson, J. (1987) J. Biol. Chem. 262, 3065–3073.
[36] Rousseau, E., Pinkos, J. and Savaria, D. (1992) Can. J. Physiol. Pharmacol. 70, 394–402.
[37] Lowry, O.H., Rosebrough, N.J., Farr, A.L. and Randall, R.J. (1951) J. Biol. Chem. 193, 265–275.
[38] Fabiato, A. (1988) Methods Enzymol. 13, 378–417.
[39] Meissner, G., Darling, E. and Eveleth, J. (1986) Biochemistry 25, 236–244.
[40] Lugnier, C., Muller, B., LeBec, A., Beaudry, C. and Rousseau, E. (1993) J. Pharmacol. Exp. Ther. 265, 1142–1151.
[41] Miller, C. (1983) Physiol. Rev. 63, 1209–1243.
[42] Decrouy, A., Juteau, M. and Rousseau, E. (1995) J. Membr. Biol. 146, 315–326.
[43] Ide, T., Morita, T., Kawasaki, T., Taguchi, T. and Kasai, M. (1991) Biochim. Biophys. Acta 1067, 213–220.
[44] Rousseau, E., Roberson, M. and Meissner, G. (1988) Eur. Biophys. J. 16, 143–151.
[45] Hals, G.D., Stein, P.G. and Palade, P.T. (1989) J. Gen. Physiol. 93, 385–410.
[46] Ehrenstein, G. and Lecar, H. (1977) Q. Rev. Biophys. 10, 1–34.
[47] Magleby, K.L. and Pallotta, B.S. (1983) J. Physiol. (London) 344, 585–604.
[48] Hill, J.A., Coronado, R. Jr. and Strauss, H.C. (1990) Am. J. Physiol. 258 (Heart Circ. Physiol. 27), H159–H164.
[49] Black, J.L., Armour, C.L., Johnson, P.R.A., Alouan, L.A. and Barnes, P.J. (1990) Am. Rev. Respir. Dis. 142, 1384–1389.
[50] Davies, N.W., Standen, N.B. and Standfield, P.R. (1991) J. Bioenerg. Biomembr. 23, 509–535.
[51] Nichols, C.G. and Lederer, W.J. (1991) Am. J. Physiol. 261 (Heart Circ. Physiol. 30), H1675–H1686.
[52] Fosset, M., De Weille, J.R., Green, R.D., Schmid-Antomarchi, H. and Lazdunski, M. (1988) J. Biol. Chem. 263, 7933–7936.
[53] Giudicelli, J.F., Richer, C. and Berdeaux, A. (1991) Presse Méd. 20, 75–81.
[54] Castle, N.A., Haylett, D.G. and Jenkinson, D.H. (1989) Trends Neurosci. 12, 59–65.
[55] Dreyer, F. (1990) Rev. Physiol. Biochem. Pharmacol. 115, 93–136.
[56] Fox, J.A. (1985) Biophys. J. 47, 573–576.
[57] Hirashima, N., Ishibashi, H. and Kirino, Y. (1991) Biochim. Biophys. Acta 1067, 235–240.
[58] Labarca, P.P. and Miller, C. (1981) J. Membr. Biol. 61, 31–38.
[59] Shen, W.K., Rasmusson, R.L., Lui, Q.-Y., Crews, A.L. and Strauss, H.C. (1993) Biophys. J. 65, 747–754.
[60] Tang, J.M., Wang, J. and Eisenberg, R.S. (1989) J. Gen. Physiol. 94, 261–278.
[61] Decrouy, A., Proteau, S. and Rousseau, E. (1995) Biophys. J. 68(2), A373.
[62] Labarca, P., Coronado, R. and Miller, C. (1980) J. Gen. Physiol. 76, 397–424.
[63] Stein, P.G., Nelson, T.E. and Palade, P.T. (1989) Biophys. J. 55, 480A.